RSC Advances

PAPER

View Article Online
View Journal | View Issue

Cite this: *RSC Adv.*, 2022, **12**, 9923

Design of choline chloride modified USY zeolites for palladium-catalyzed acetylene hydrochlorination†

Zeqing Long,‡[a] Lu Wang,‡*[a] Haijun Yan,[a] Jianxin Si,[a] Meng Zhang,[a] Jide Wang,[a] Ling Zhao,[ab] Chao Yang[a] and Ronglan Wu[a]

Received 21st February 2022
Accepted 24th March 2022

DOI: 10.1039/d2ra01142e

rsc.li/rsc-advances

USY zeolites (USY) were applied to design and synthesize palladium-based heterogeneous catalysts for exploring an efficient non-mercuric catalyst for acetylene hydrochlorination. Choline chloride (ChCl) was selected as the nitrogen-containing ligand to modify the Pd@USY catalysts and the proposed Pd@15ChCl@USY catalyst exhibited obviously the best catalytic performance with a stable acetylene conversion and vinyl chloride selectivity of over 99.0% for more than 20 h. According to the results of characterization and the density functional theory calculations, it is indicated that the addition of ChCl can significantly inhibit the agglomeration and loss of the Pd active species, prevent carbon deposition and enhance the ability of HCl and C_2H_2 adsorption and C_2H_3Cl desorption, resulting in promoting the catalytic performance of Pd@USY catalysts during the acetylene hydrochlorination reaction.

1 Introduction

Polyvinyl chloride (PVC) is one of the five universal engineering resin materials in the world, which has the advantages of low price, flame retardance, high strength, good weather resistance and excellent processability, and is widely used in industry, agriculture, construction, daily necessities, and other industries.[1–3] Industrially, PVC is produced primarily by the polymerization of vinyl chloride monomer (VCM). At present, the production methods of VCM are the acetylene, ethylene and ethane methods.[4] Because of the energy structure of our country, the synthesis process of VCM is acetylene hydrochlorination method. However, the traditional $HgCl_2$/AC catalyst is toxic and easy to sublimate, which seriously endangers the ecological environment and human health, coupled with the global shortage of mercury resources, so that the PVC industry is facing the dual pressure of mercury pollution and a shortage of mercury resources.[1,5,6] In order to eliminate mercury consumption in the PVC industry by 2025, as scheduled in the Minamata Convention.[7] The development of more effective and stable non-mercury catalysts is essential to the sustainable development of the chlor-alkali industry.

In recent decades, a series of mercury-free catalysts for acetylene hydrochloride has been explored, such as Au,[8,9] Ru,[10,11] Pt,[12,13] and Cu,[14,15] Bi,[16,17] *etc.* Gold (Au)-based catalysts are the most widely used and studied owing to their unprecedented intrinsic activity in this reaction.[18–20] Despite the commercial success of gold-based catalysts ($Na_3Au(S_2O_3)_2$/C),[1] there is still ongoing research to find alternative catalysts for industrial applications. As far as Ru-based catalysts are concerned, the coexistence of abundant Ru species with distinct valence states (such as RuO clusters, RuO_2, RuO_x and cationic $RuCl_x$ species) on the carrier surface makes it difficult to identify the individual catalytic behaviour of each Ru species.[11,21] In this regard, Pd species with relatively simple valence state (II and 0) may be another more potentially promising candidate to replace Au- and Ru-entities derived catalysts.[22,23] In recent years, zeolites have been widely applied in the petrochemical industry due to their good hydrothermal stability, rich pore structure, large surface area, and adjustable acidity, which can play the role of screening and catalysis.[24–26] For acetylene hydrochlorination, Liu *et al.* reported a systematic study of the activity of 13X zeolite without loading any active metal component, when the reaction temperature is over 300 °C, the conversion of acetylene is close to 100% and the selectivity of vinyl chloride is over 90.0%; besides, the spent catalyst can be partially regenerated by calcination and they believe that the activity of 13X molecular sieve is related to its unique zeolite structure.[27] Li *et al.* also reported that an efficient and stable heterogeneous zeolite supported ionic liquid catalyst (IL/CaX) has been explored in acetylene hydrochlorination reaction, which exhibits an excellent catalytic performance when compared to the Au/C catalyst.[28]

[a]*Key Laboratory of Oil and Gas Fine Chemicals, Ministry of Education, Xinjiang Uyghur Autonomous Region, School of Chemical Engineering and Technology, Xinjiang University, Urumqi 830017, China. E-mail: wanglu_4951@163.com; Fax: +86-0991-8581018; Tel: +86-0991-8581018*

[b]*State Key Laboratory of Chemical Engineering, School of Chemical Engineering, East China University of Science and Technology, Shanghai 200237, China*

† Electronic supplementary information (ESI) available. See DOI: 10.1039/d2ra01142e

‡ The two authors contributed equally to this work.

In our previous work, Pd-supported Y zeolite (Pd/HY) catalysts with 0.5 wt% Pd content were prepared by ultrasound-assisted impregnation and investigated in a fixed bed reactor at 160 °C, $V(HCl)/V(C_2H_2) = 1.25$ and gas hourly space velocity of $C_2H_2 = 110\ h^{-1}$. For the Pd/HY catalyst, the conversion of acetylene is more than 95.0% and the selectivity of vinyl chloride is over 90.0% during 2 hours, which proved that the Pd metal can be the active metal for acetylene hydrochlorination, although Pd-based catalysts are easy sintered and deactivated.[29] After that, we modified the supports (NH_4F,[30] NH_4F-urea,[31] boron[32]) to improve the anti-sintering of palladium and the results showed that heteroatom modifications may be an effective strategy to improve properties of catalysts for increasing the dispersion of the Pd species and reducing their particle sizes to improve the sintering resistance of the Pd-based catalyst. Ionic liquids (ILs) have attracted much attention due to their unexpected catalytic activity in many heterogeneous reactions in recent years,[15,33–35] especially in the acetylene hydrochlorination reaction.[34–42] Li *et al.* synthesized pyridinic N-rich aromatic ladder structure catalysts through controlling the self-assembly of polyacrylonitrile polymer chains and the prepared catalysts showed ~93.0% acetylene conversion and exhibited a satisfying stability during 200 h.[36] Zhao *et al.* prepared nitrogen–phosphorus doped carbon catalysts using 1-ethylsulfonic acid-3-methylimidazolium dihydrogen phosphate [$ESO_3HMim + H_2PO_4^-$] and 1-ethyl-3-methylimidazolium dicyandiamide [$[EMim]^+N(CN)_2^-$] as phosphorus and nitrogen sources, and the catalyst also has an excellent activity for acetylene hydrochlorination.[34] Zhang *et al.* successfully synthesized Ru-10% DMPU/AC catalysts and suggested the anchoring effect of the N-containing ligand can increase the dispersion of Ru species and decrease the coke deposition during reaction.[38] Compared with Ru/AC, series of quaternary ammonium ionic liquids (QAIL) modified Ru-QAILs/AC catalysts revealed the synergistic effect between metal and support and improve the catalytic performance of catalysts, but their high cost limits their application in PVC industry.[39,40] Besides, choline chloride (ChCl) is cheaper, more non-toxic, greener and easier to store than most ionic liquids, which has been widely used in the Diels–Alder reaction and the Fischer indole cyclization reaction.[41–44] Therefore, we hypothesized that ChCl could improve the performance of Pd@USY zeolite catalyst in acetylene hydrochlorination as well.

In this work, a mercury-free Pd-based@USY catalyst with high efficiency by ChCl modification was designed and developed. The ChCl additive had great influence on the catalytic performance of Pd-based@USY catalyst and the promotion effects of ChCl were studied systematically by a series of experimental characterizations combined with density functional theory (DFT) calculations. This work created a novel way for the modified strategies for mercury-free Pd-based@USY catalysts in acetylene hydrochlorination reaction, which also can improve the sustainable development of PVC industry.

2 Experimental

2.1. Catalyst preparation

The supported Pd@ChCl@USY catalysts were prepared using an ultrasonic-assisted impregnation method and USY zeolite (20–40 mesh, Si/Al = 6) purchased from Nankai University Co., Ltd. Take the preparation method of Pd@1ChCl@USY catalyst for example. Firstly: 0.04 g palladium chloride precursor ($PdCl_2$, purity 59% purchased from Shanghai Titan Scientific Co., Ltd) and 0.75 g choline chloride (ChCl purity ≥ 98%, purchased from Shanghai Titan Scientific Co., Ltd) were dissolved in 6.32 ml hydrogen chloride aqueous solution (HCl purity ≥ 99.99%) and deionized water, and the mixture was stirring and completely dissolved at room temperature. Then, 5.0 g USY zeolite was added with vigorous stirring and the obtained system was in an ultrasonic bath for 1 h. Finally, the obtained sample was placed under atmosphere condition for 10 h and dried at 120 °C for 8 h, denoted as Pd@ChCl@USY where 1 represents the mass percentage of ChCl. Similar methods were applied to prepare the Pd@USY, ChCl@USY and Pd@*x*ChCl@USY catalysts the serious of Pd@*x*ChCl@USY catalysts with the mass ration of 5%, 10%, 15%, and 20% ChCl species were named as Pd@5ChCl@USY, Pd@10ChCl@USY, Pd@15ChCl@USY, and Pd@20ChCl@USY, respectively and the load of Pd was kept content at 0.5% in all catalysts. The Pd–ChCl@USY and the ChCl–Pd@USY catalysts were also prepared by ultrasonic-assisted impregnation method. The Pd–ChCl@USY catalyst was made through by first impregnating $PdCl_2$ precursor(aq) on USY zeolite followed by impregnating ChCl(aq) on Pd@USY after drying at 120 °C for 8 h. The preparation of the ChCl–Pd@USY catalyst was similar to the route of the Pd–ChCl@USY catalyst but the impregnation order of $PdCl_2$ precursor and ChCl solution was reversed. Besides, 0.5 wt% Pd and 15 wt% ChCl were contained in all two catalysts.

2.2. Catalytic performance evaluation

All catalysts (5.0 g) were evaluated into the self-designed quartz (tube 10 mm diameter, 40 mm length), purged with N_2 (15 ml min^{-1}) to remove water and air activated under hydrogen chloride (15 ml min^{-1}) atmosphere at 160 °C for 40 min, then reacted under the flow of hydrogen chloride (5.2 ml min^{-1}) and acetylene (7.2 ml min^{-1}) at 160 °C (feed volume ratio V_{HCl}:$V_{C_2H_2}$ = 1.25), the C_2H_2 gas hourly space velocity of 120 h^{-1}. The acetylene conversion (X_A) and vinyl chloride selectivity (S_{vc}) were analyzed by a gas chromatography (GC 2010 Shimadzu, Kyoto, Japan) after eliminating unreacted hydrogen chloride or other effluent gases.

2.3. Catalyst characterization

Scanning transmission election microscopy (STEM) and transmission electron microscopy (TEM) were measured by JEM-2100F (JEOL, Japan) the acceleration voltage of 200 kV. The elemental composition was achieved by an energy dispersive X-ray spectroscopy (EDS, JEM-2100F) device coupled to STEM. X-ray diffraction (XRD, X'Pert PRO MPD) was carried out to determine dispersity and crystallinity of the active component in prepared catalysts with Cu-Kα radiation (λ = 0.15407 nm) irradiation over the range $10° \le 2\theta \le 80°$. X-ray photoelectron spectroscopy (XPS, Thermo ESCALAB250XI) was performed to analyze the chemical elements valence states of the catalysts,

and the standard C 1s (284.8 eV) was employed. Inductively coupled plasma optical emission spectroscopy (ICP-OES, Agilent ICP-OEST30) was detected to distinguish the actual Pd loading for catalysts. Brunner–Emmet–Teller (BET, Quanta chrome Auto sorb iQ2) was measured to the various texture parameters of the prepared catalysts, which were pretreated at 120 °C for 5 h and tested at liquid nitrogen temperature (−196 °C). Thermogravimetric analysis (TGA, Thermo Plus EVO2) was conducted to evaluate the thermostability and carbon deposition of catalysts under 100 ml min^{-1} air gas flow and a heating rate of 10 °C min^{-1} from 30–800 °C. Ammonia temperature programmed temperature desorption (NH_3-TPD, AutoChem II 2920) tests were over the range from room temperature to 700 °C at a heating rate of 10 °C min^{-1} for investigating the acidic properties of catalysts and pyridine adsorption infrared spectra (Py-IR, Tensor 27) were obtained from 1000 to 2000 cm^{-1}. Besides, acetylene temperature programmed desorption (C_2H_2-TPD), hydrogen chloride temperature programmed desorption (HCl-TPD) and vinyl chloride temperature programmed desorption (C_2H_3Cl-TPD) test were carried out using a AutoChem II 2920 adsorption Instrument and the procedure was as follow: the sample (0.75 mg) was treated with C_2H_2, HCl or C_2H_3Cl at 180 °C for 2 h initially, then adsorption and sweeping under 100 ml min^{-1} Ar (purity, 99.9%) gas flow and a heating range of 10 °C min^{-1} from 25 °C to 800 °C.

2.4. Density functional theory (DFT) simulation

All the density functional theory (DFT) calculations were carried out using the Vienna *ab initio* Simulation Package (VASP).[45,46] The generalized gradient approximation (GGA) with Perdew–Burke–Ernzerhof (PBE) formulation has been employed to define the correlation energy and electron exchange. A 2 × 2 × 1 *k*-point set and a 400 eV energy cut-off had been used for the optimized structures.[47–49] The vacuum region (15 Å), the energy of the convergence criteria (10^{-5} eV) and the force of the convergence criteria (0.04 eV $Å^{-1}$) were constructed. Then the adsorption energies (E_{ads}) were calculated as $E_{ads} = E_{ad/sub} - E_{ad} - E_{sub}$, where $E_{ad/sub}$, E_{ad}, and E_{sub} are the total energies of the optimized adsorbate/substrate system, the adsorbate in the structure, and the clean substrate, respectively. $U = 4.01$ eV was applied to Pd states in our calculations.

3 Result and discussion

The catalytic performances of USY, ChCl@USY, Pd@USY and Pd@ChCl@USY catalysts for acetylene hydrochlorination are displayed in Fig. 1 and S1.† Over the USY and ChCl@USY (Fig. 1a), the negligible catalytic activity (less than 8.9%) was observed obviously indicating that USY support and ChCl additive have little contribution to the reaction activity. After loading Pd species, Pd@USY and Pd@ChCl@USY catalysts were all exhibited a certain activity attributed to the contributions of Pd species. For Pd@USY catalyst, the acetylene conversion decreased from 74.8% to 15.0% during the reaction, showing the Pd@USY catalysts was active but the poor stability. For Pd@ChCl@USY catalyst, it is observed the significantly increasing activity and stability (the acetylene conversion was exhibited approximately 99.6% during the reaction), which proved that the ChCl addition can effectively improve the catalytic performance Pd@USY catalyst. The catalytic performance Pd–ChCl@USY and ChCl–Pd@USY catalysts had similar and stable conversion but longer induction period during 600 min, and the co-impregnation was the optional method for the Pd@ChCl@USY catalyst (Fig. S2†). In view of amount of ChCl additives, the effect of ChCl additives on the catalytic activity may be sorted in the following order: Pd@15ChCl@USY (99.9%) > Pd@20ChCl@USY (96.0%) > Pd@10ChCl@USY (90.9%) > Pd@5ChCl@USY (85.0%) > Pd@1ChCl@USY (80.0%) (Fig. 1b). In addition, All the prepared Pd@ChCl@USY-based catalysts showed more than 99.8% vinyl chloride selectivity. Especially, the Pd@15ChCl@USY catalyst exhibited the optimal catalytic performance, the maximum C_2H_2 conversion was kept above 99.5% during 20 h (Fig. 1c). So, it is suggested the appropriate amount of ChCl additive can both enhance the catalytic activity and selectivity of Pd@USY-based catalysts for acetylene hydrochlorination.

EDS mapping and STEM images of the fresh Pd@15ChCl@USY catalyst were showed in Fig. 2. It was demonstrated that the C, N, Pd, Cl, Si, Al and O signals (Si Al and O elements were attributed to the original USY zeolite) were homogeneously distributed over the catalyst, confirming the Pd species and ChCl additives were successfully doped into the USY zeolite. From Fig. 3, the characteristic diffraction peaks at 10.3° (220), 12.1° (311), 15.9° (331), 19.0° (511), 20.8° (440), 24.1° (533), 27.6° (642), and 30.0° (555) belonged to the characteristic

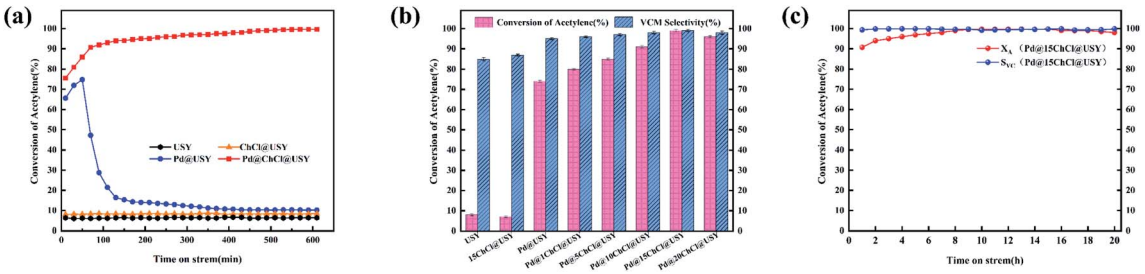

Fig. 1 Conversion of acetylene of USY-based catalysts (a); catalytic performance of the Pd@ChCl@USY catalysts with different ChCl mass ratios (b); catalytic performance of the Pd@15ChCl@USY catalyst (c). Reaction conditions: $T = 160$ °C, GHSV(C_2H_2) = 120 h^{-1}, and V(HCl):V(C_2H_2) = 1.25.

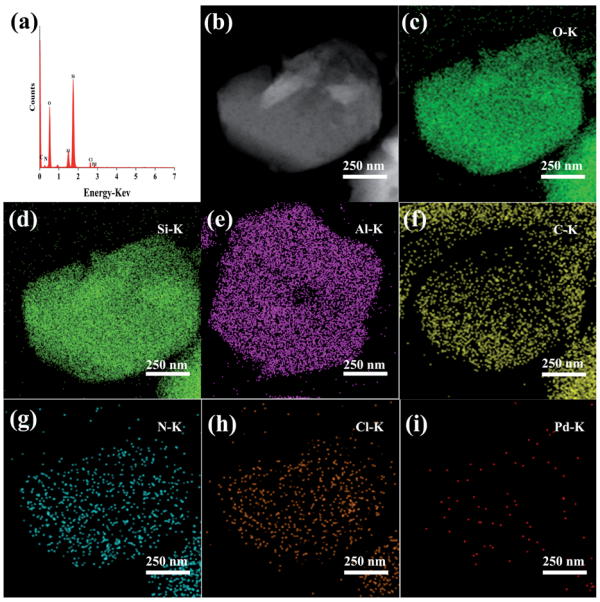

Fig. 2 EDS analysis (a), STEM image (b) and elemental mapping images (c–i) of the fresh Pd@15ChCl@USY catalyst.

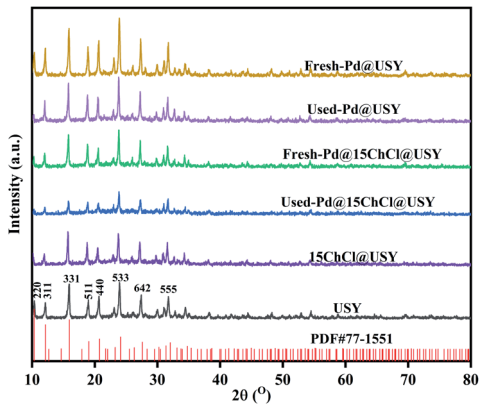

Fig. 3 XRD patterns of Pd-based@USY catalysts.

peaks of USY (JCPDS no. 77-1551) were observed all the fresh and used cata-lysts, but no discernible reflections of Pd species were detected in all the prepared Pd-based@USY catalysts, which indicated that the active sites of Pd species were highly dispersed on the USY-based support, or the crystalline size of Pd species was below the limit of XRD detection (<4–5 nm), or the low loading of Pd.[50,51] HRTEM images (Fig. 4) was carried out to observe the palladium particle size distribution of the fresh and used Pd@USY and Pd@15ChCl@USY catalysts. For the fresh catalysts (Fig. 4a and c), there appear almost no Pd dusters or nanoparticles on all USY-based supports, indicating the highly dispersed palladium particles,[52–54] which is consistent with the XRD analysis (Fig. 3). Compared with the fresh catalysts, Pd nanoparticles were detected in the used Pd@USY and Pd@15ChCl@USY catalysts, as observed in Fig. 4b and d. In addition, one characteristic lattice fringes with lattice spacings of 0.23 nm are found in the used Pd@USY HRTEM images

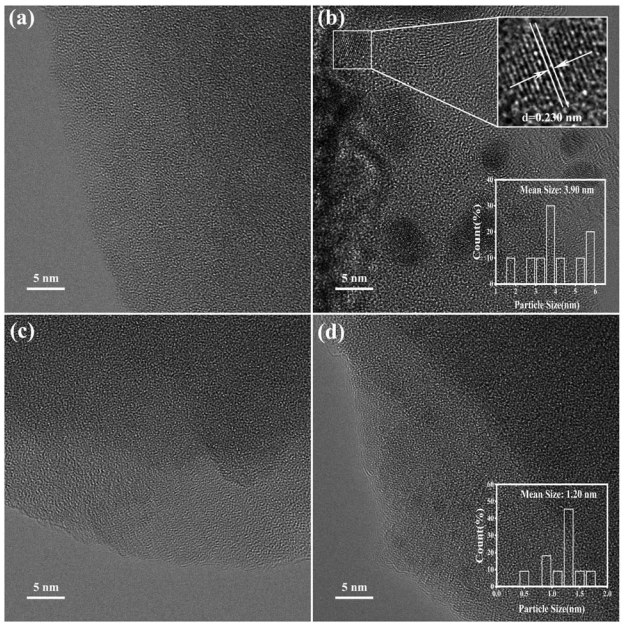

Fig. 4 HRTEM images of the fresh Pd@USY (a), used Pd@USY (b), fresh Pd@15ChCl@USY (c) and used Pd@15ChCl@USY (d).

(Fig. 4b), which can be attributed to the (111) crystal faces of palladium with an average size of about 3.9 nm, manifesting the sintering of the Pd metal on the catalyst during the reaction and is also one reason for the rapid activity decrease of the Pd@USY catalyst.[13,55] However, less and smaller (about 1.20 nm) visible Pd nanoparticles are detected in the Pd@15ChCl@USY HRTEM images (Fig. 4d) which can be suggested that although the aggregation of Pd species are in the used Pd@15ChCl@USY catalyst as well, the appropriate ChCl treatment during the catalyst preparation and reaction processes can limit the aggregation of Pd active species, which is favorable for continuous high activity and stability of the catalysts for acetylene hydrochlorination.

Fig. 5a–d displays the XPS curves of the Pd (3d) region for the fresh and used Pd@USY and Pd@15ChCl@USY, and all Pd (3d) signals could be well deconvoluted into Pd^{2+} (about 337.1 eV and 342.2 eV) and Pd^{0} (about 335.5 eV and 340.6 eV) species.[13,56] The relative contents of Pd^{0} and Pd^{2+} species in Pd-based catalysts obtained from XPS are listed in Table 1. For the fresh catalysts, it can be seen that Pd^{2+} species acts as the main active component for acetylene hydrochlorination drawn by other researchers.[52,57] And there is a slight difference between the palladium component before and after adding ChCl in the XPS results, which further proves that ChCl addition couldn't directly affect the valence states of the Pd species in the catalysts. Compared with the fresh catalysts, it indicated that the Pd^{2+}/Pd^{0} ratio in the used catalysts was significantly decreased, suggesting that the active Pd^{2+} species had been reduced during the reaction resulted in the decreased activity of the catalysts. However, a slower reduction ($Pd^{2+} \rightarrow Pd^{0}$) were found in the Pd@15ChCl@USY catalysts experiences when compared with the Pd@USY catalysts, which is likely one of reasons for the better catalytic performance in Pd@15ChCl@USY catalysts. On

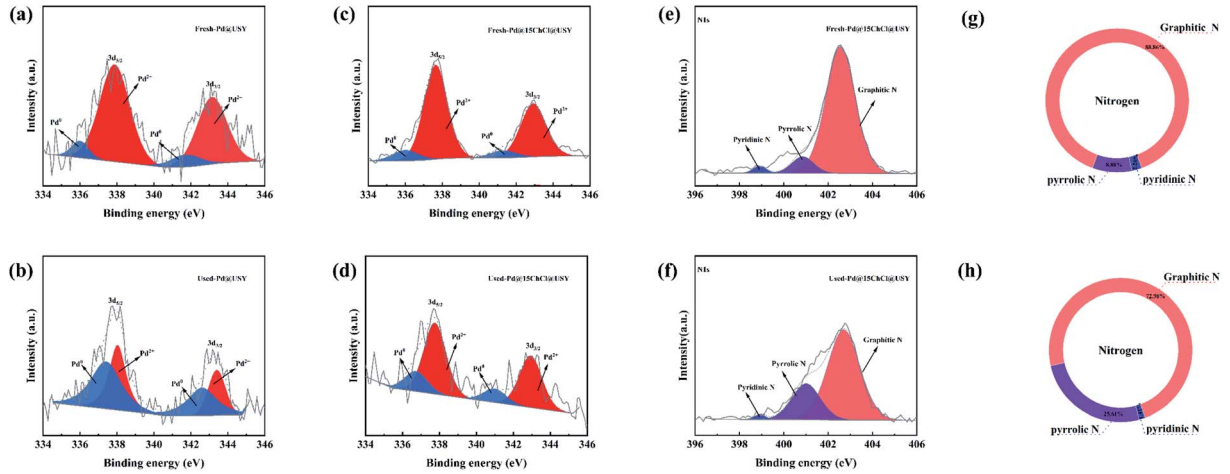

Fig. 5 XPS images and results of the Pd-based@USY catalysts before and after reaction: Pd spectra and corresponding Pd contents of the fresh Pd@USY (a), used Pd@USY (b), fresh Pd@15ChCl@USY (c and e) and used Pd@15ChCl@USY (d and f); N spectra and corresponding N contents of the fresh Pd@15ChCl@USY (g) and used Pd@15ChCl@USY (h).

Table 1 The relative content of Pd species in the fresh and used catalysts determined by XPS and the actual Pd content determined by ICP

Catalysts	Pd^0 (area %)	Pd^{2+} (area %)
Fresh-Pd@USY	11.83	88.17
Used-Pd@USY	55.37	44.63
Fresh-Pd@15ChCl@USY	11.66	88.34
Used-Pd@15ChCl@USY	21.85	78.15

Catalysts	Total Pd (wt%)		Loss ratio of Pd (%)
	Fresh	Used	
Pd@USY	0.63	0.21	58.73
Pd@15ChCl@USY	0.63	0.41	34.92

the basis of these results, it concluded that the existence of ChCl (Fig. 2 and S3†) act as a stabilizer to inhibit the reduction of Pd^{2+} species, thus effectively prolong the lifetime of the Pd@USY catalyst for acetylene hydrochlorination. Additionally, it was clearly seen that three individual peaks at 398.8 eV, 401.0 eV and 402.5 eV, demonstrating the coexistence of pyridinic N, pyrrolic N and graphitic N respectively in fresh and used Pd@15ChCl@USY catalysts (Fig. 5e and f). Moreover, their relative contents of the existing nitrogen species according to XPS were show in Fig. 5g and h. For the Pd@15ChCl@USY catalyst, it suggested that the type of nitrogen species had no changes but the relative contents before and after reaction, especially pyridinic N and graphitic N. Although the role of various N species is still under debate in the metal-based catalysts, N-containing species could be positive to the election transferred from N species to the active center, thus enhancing the catalytic activity.[50,58–60]

In order to further study the apparent influence of ChCl for the loss active component, ICP data of the amounts of the Pd in the fresh and used Pd-based catalysts are detected (Table 1). Compared to the fresh catalysts, an obvious decrease in Pd content is shown in all the used catalysts, indicating that the Pd species were lost during the reaction. Meanwhile, it can be observed that the loss ratio of Pd species in the Pd@15ChCl@USY catalyst (34.92%) was much less than that in the Pd@USY catalyst (58.73%), suggesting that ChCl addition in the in the Pd@15ChCl@USY catalyst stabilized Pd species and decreased Pd loss during the reaction, resulting in better catalytic activity.

Table 2 show the structure and texture parameters of the fresh and used Pd@USY and Pd@15ChCl@USY catalysts. It can be seen that the bare USY possesses the highest BET specific surface area (S_{BET}) and the total pore volume (V) of 689 $m^2\ g^{-1}$ and 0.41 $cm^3\ g^{-1}$, respectively. However, the S_{BET} and V of all the fresh Pd-based catalysts substantially decrease with the adding of Pd and ChCl species, which may occupy some of the available space, what's more, the S_{BET} and V of the fresh Pd@15ChCl@USY catalyst was lower that of the Pd@USY catalyst and the ChCl with coordination with Pd^{2+} has been polymerized, which blocked the pores of catalysts and changed pore structure.[15,61,62] After reaction, the S_{BET} and V of all used catalysts were much lower than those of the fresh catalysts, resulting in the carbon deposition or polymerization of the reactant acetylene or the product vinyl chloride for decrease of

Table 2 Porous structure parameters of catalysts

Catalysts	$S_{BET}{}^a$ ($m^2\ g^{-1}$)	V^b ($cm^3\ g^{-1}$)	D^c (nm)
USY	689	0.41	2.47
Fresh-Pd@USY	573	0.32	2.36
Used-Pd@USY	61	0.10	6.33
Fresh-Pd@15ChCl@USY	71	0.12	7.06
Used-Pd@15ChCl@USY	35	0.06	6.82

[a] Specific surface area. [b] Total pore volume. [c] Average pore diameter.

the catalytic the catalytic activity. Data analysis indicated that the relative loss of S_{BET} (S_{BET}%) during the reaction was in the order of Pd@15ChCl@USY (51.42%) < Pd@USY (89.35%), revealing that the existence of ChCl species may be conducive to the rapid reaction of acetylene hydrochlorination and inhibits the possibility of the carbon formation.

The degree of carbon deposition on the surface of palladium-based catalysts are detected by TGA and the mass loss of fresh and used Pd@USY and Pd@15ChCl@USY catalysts are compared in Fig. 6. Obvious, the Pd-based catalysts showed a visible mass loss before 150 °C, owing to the evaporation of moisture or other adsorbed species (like water) on the catalyst surface.[9] A significant weight loss between 150 °C and 450 °C could mainly attribute to the burning of the carbon deposition and when the temperature is above 450 °C the USY support combustion.[32,63] Based on the contrastive method,[64] the carbon deposition of the Pd@15ChCl@USY catalyst could be calculated as 1.91%, which was 51.77% less than that of the Pd@USY catalyst (3.96%), providing indirect evidence for the formation of the carbon deposition on the catalyst surface and it is the other reason for the deactivation of the Pd-based catalysts. In addition, it also indicated that the ChCl addition could inhibit the formation of the carbon deposition effectively on the catalyst surface during the reaction.

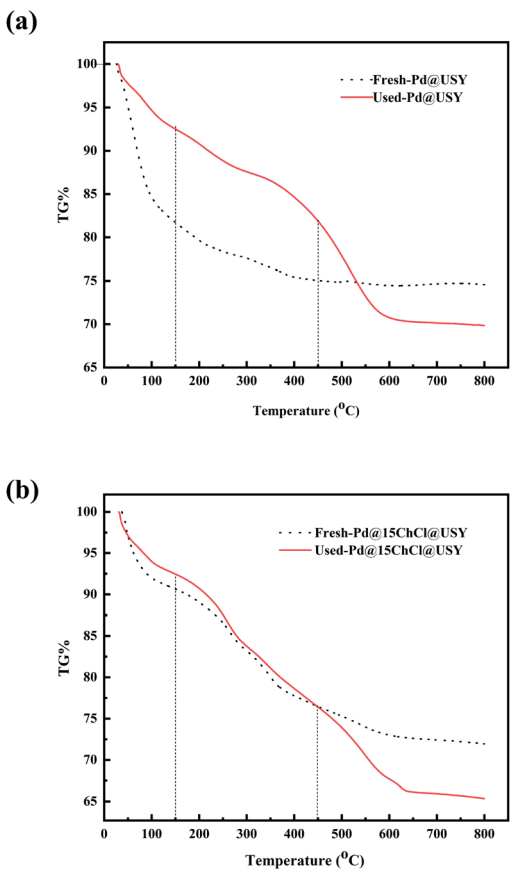

Fig. 6 TGA profiles of the Pd@USY (a) and Pd@15ChCl@USY (b) catalysts.

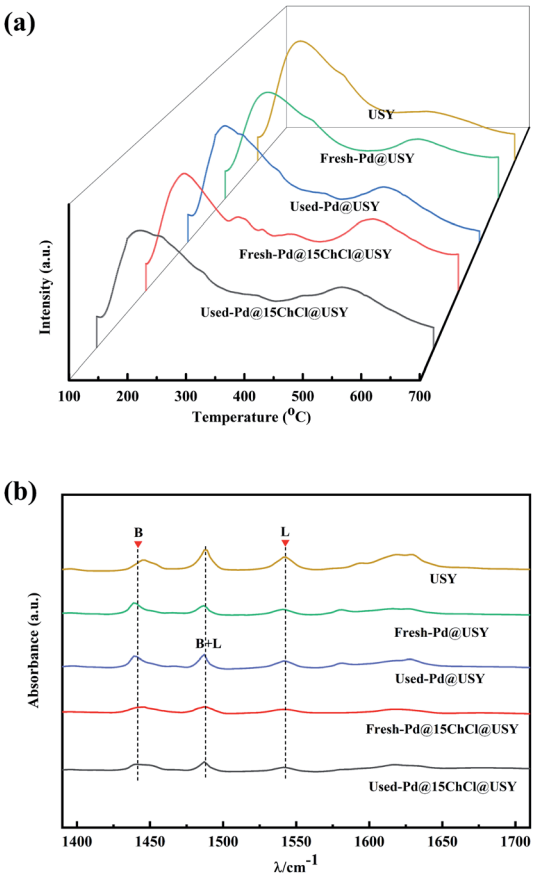

Fig. 7 NH_3-TPD profiles of the Pd-based catalyst (a) and pyridine adsorption IR of the Pd-based catalyst (b).

NH_3-TPD profiles of all samples are displayed in Fig. 7a and the profile of the USY support is provided for comparison. As can been seen, all samples showed the ammonia desorption peaks centered at around 200 °C was ascribed to the weak acid sites (Lewis) and at around 500 °C related to the strong acid sites (Brønsted).[24,26,65,66] Compared with the pure USY support, it was clearly exhibited that the intensities of weak acid sites were decreased, and the strong acid sites were increased by the incorporation of Pd metal and ChCl additive into the USY zeolite, indicating the decreased amount of the weak acid sites and the increased amount of the strong acid sites. In addition, the fresh Pd@15ChCl@USY catalyst showed more strong acid sites than the fresh Pd@USY catalyst, which might be associated with the framework dealumination and the presence of nitrogen species.[67,68] After reaction, both the intensities of the weak and strong acid sites on the used Pd@USY and Pd@15ChCl@USY catalysts were decreased, which provided further clarification that both amounts and strength of the strong acid sites in Pd-based@USY catalyst is generally accepted to improve the catalytic performance for acetylene hydrochlorination.[32,63]

Fig. 7b reports the 1400–1600 cm^{-1} Py-IR spectra to distinguish the types of surface acid sites further. The result indicated that indicated that Py-IR bands centered at 1450 cm^{-1}, 1540 cm^{-1} and 1490 cm^{-1} were correspond to Lewis (L),

Brønsted (B) and both Brønsted and Lewis (B + L) acid sites, respectively.[69–71] According to quantitative analysis of the Brønsted/Lewis (B/L) acidity radio for each catalyst at the temperature 160 °C was shown in Table S1.† The B/L acidity radio of the fresh Pd@15ChCl@USY catalyst was remarkably higher than that of the fresh Pd@USY catalyst and the pure USY support under the same condition, suggesting that more abundant Brønsted acid sites on the fresh Pd@15ChCl@USY catalyst (as indicated in the NH_3-TPD results) related to the ChCl additive. Combined with the catalytic performance of Pd-based catalysts (Fig. 1), it is also reasonable to attribute the enhanced catalytic activity of Pd@15ChCl@USY catalyst to the more amount of surface B acid sites.

The introduction of ChCl additive affects the electronic properties of the Pd active species and adsorption ability of the fresh catalyst for the HCl and C_2H_2 reactants, which is directly related to its catalytic performance in acetylene hydrochlorination reaction.[68,72] So, the HCl-TPD and C_2H_2-TPD experiments were carried out to investigate the adsorption ability of the fresh Pd@USY and Pd@15ChCl@USY catalysts (Fig. 8a and b) For the HCl-TPD curves (Fig. 8a), Pd@15ChCl@USY catalyst exhibited a similar profile (the multistate-adsorbed HCl at the central temperatures around 160 °C and 450 °C) compared to the Pd@USY catalyst. According to the qualitatively analysis by the area of the desorption peaks, it is suggested that the order of the adsorption capacities was Pd@15ChCl@USY > Pd@USY, which indicated that the coordination of the Pd species and ChCl ligand may improve the electron transfer from H to Pd(II) species, resulting in the increase electron density around the Pd active and enhanced the HCl adsorption.[73] In terms of C_2H_2-TPD curves, the Pd@USY and the Pd@15ChCl@USY catalysts also showed a multistate-adsorbed C_2H_2 at the central temperature around 160 °C and 450 °C (Fig. 8b). As shown in Fig. 8b, two desorption peaks are present for acetylene desorption from both Pd@USY and Pd@15ChCl@USY catalysts in Fig. 8b, where the weaker peaks covering the temperature ~150 °C correspond to the C_2H_2 desorption from the USY support, while the stronger peaks at temperatures about 450 °C were attributed to the C_2H_2 desorption from cationic Pd species.[33,74] In addition, the complexation of the Pd species and the ChCl ligand had a negligible effect on the desorption temperature of C_2H_2, but it clearly enhanced the C_2H_2 adsorption amount, which was in agreement with the order of catalytic performance of the catalysts (Fig. 1).[75] Combined with the HCl-TPD and C_2H_2-TPD data, it is well shown that the incorporation of ChCl can improve the adsorption ability of the Pd@USY catalyst to both the HCl and C_2H_2 reactants, which is beneficial to the catalytic reaction. Moreover, C_2H_3Cl-TPD experiments were performed to further study the effect of the presence of ChCl ligand on the adsorption ability of C_2H_3Cl product. It is well known that the peak area indicates the adsorption capacity and the desorption temperature reflects the adsorption strength.[76] As shown in Fig. 8c, the adsorption capacity for C_2H_3Cl on the Pd@15ChCl@USY catalyst was lower than that on the Pd@USY catalyst. At the same time, we found that the C_2H_2 desorption peak of Pd@ChCl@USY catalyst at 450 °C was lower than that of Pd@USY catalyst at 500 °C, which suggested that the addition of ChCl decreased the adsorption of C_2H_3Cl on Pd@USY and made the C_2H_3Cl desorption on Pd@ChCl@USY easier. According to the results of TPD, the presence of ChCl can strengthen the reactants adsorption and the product desorption, resulting in the enhanced catalytic performance of the Pd@15ChCl@USY catalyst for acetylene hydrochlorination.[76,77]

In order to further investigate the effect of ChCl ligand on the electronic property and adsorption ability of Pd active species, DFT calculations were performed and the optimized ground-state structures of the reactants are shown in Fig. 9. The adsorption energy of C_2H_2 and HCl on Pd@15ChCl@USY were calculated at −0.85 eV and −0.72 eV and that on Pd@USY catalyst were calculated at −0.55 eV and −0.41 eV, respectively. Compared to the Pd@USY catalyst, it is proved that the Pd@15ChCl@USY catalyst owned the stronger the adsorption capacity of the reactants (C_2H_2 and HCl), which was in favor of the catalytic reaction. However, the adsorption energy of C_2H_3Cl on Pd@15ChCl@USY catalyst (−0.32 eV) was lower than that on Pd@USY (−0.73 eV), indicating that Pd@15ChCl@USY was more favor −0.72 eV and that on Pd@USY catalyst were calculated at −0.55 eV and −0.41 respectively. Compared to the Pd@USY catalyst, it is proved that the Pd@15ChCl@USY catalyst owned the stronger the adsorption capacity of the reactants (C_2H_2 and HCl), which was in favor of the catalytic reaction. However, the adsorption energy of C_2H_3Cl on Pd@15ChCl@USY catalyst (−0.32 eV) was lower than that on Pd@USY catalyst (−0.73 eV), indicating that Pd@15ChCl@USY was more favorable for the product desorption. Thus, the DFT theoretical simulation results were basically consistent with the experimental results of TPD

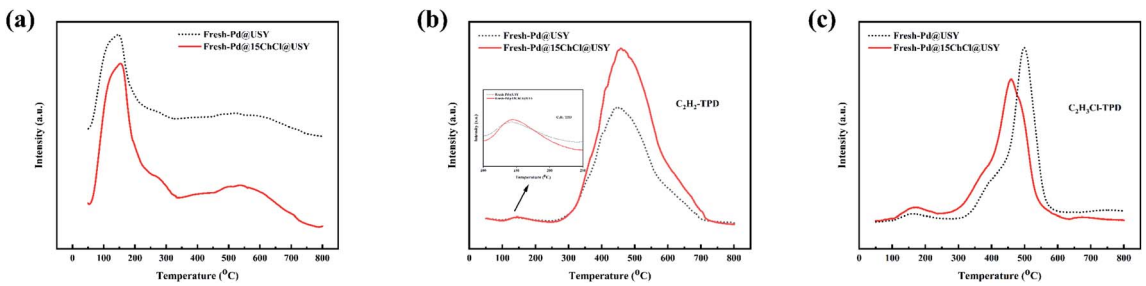

Fig. 8 TPD evolution profiles of the Pd-based catalysts for the desorption of HCl (a), C_2H_2 (b) and C_2H_3Cl (c).

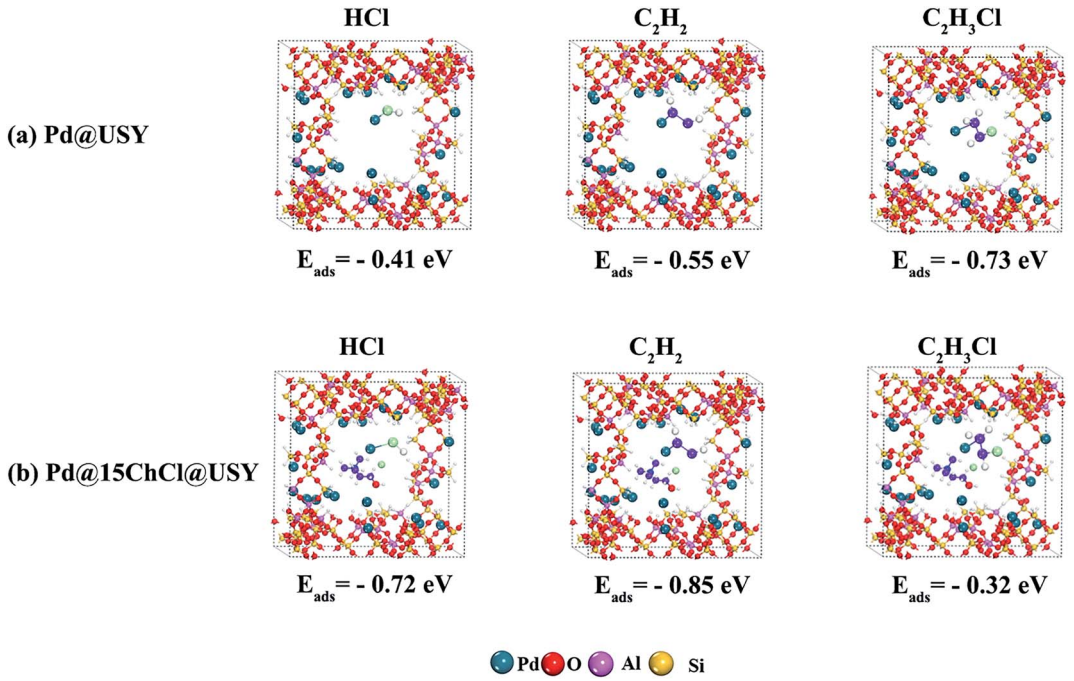

Fig. 9 Adsorption energy of HCl, C_2H_2 and C_2H_3Cl on Pd@USY catalyst (a) and Pd@15ChCl@USY catalyst (b).

results (Fig. 8). Moreover, the stronger adsorption of C_2H_2 than HCl on Pd@USY (Fig. 9a) or Pd@15ChCl@USY (Fig. 9b) showed the necessity of C_2H_2 adsorption for triggering this reaction, suggesting the reaction was triggered by the adsorbed C_2H_2, followed by linking HCl to its optimized ground-state structure, giving rise to the generation and C_2H_3Cl desorption as a whole reaction process, which followed a typical Eley–Rideal (E–R) mechanism.

4 Conclusions

ChCl modified Pd@USY catalysts were synthesized and assessed for acetylene hydrochlorination. The results showed that the addition of the chlorine chloride can effectively improve the activity and stability of the Pd@USY catalyst, and the proposed Pd@15ChCl@USY catalyst exhibited obviously better catalytic performance under the same reaction conditions, with acetylene conversion and VCM selectivity over 99% more than 20 h. The characterization results indicated that the interaction between the central Pd active species and the ChCl additive guaranteed the anchoring and high dispersion of Pd active species on the surface of catalysts. Furthermore, the ChCl ligand relatively discouraged the agglomeration and loss of active species, inhibited the carbon deposition and stabilized the Pd species in a high-valent state, thus significantly slowing down the deactivation of the catalyst. In particular, the presence of ChCl ligand also made Pd^{2+} harder to reduce the Pd species, which synergistically enhanced the adsorption and activation ability of HCl and C_2H_2 reactants and the desorption ability of C_2H_3Cl products, resulting in Pd@ChCl@USY catalysts with enhanced activity and long-term stability. This current work not only broadens the scope of Pd-based catalysts but also deepens the understandings of the modified strategies for mercury-free catalysts in acetylene hydrochlori-nation reaction.

Author contributions

Zeqing Long: investigation, methodology, data curation, formal analysis, writing – original draft. Lu Wang: investigation, methodology, funding acquisition, project administration, supervision, writing – review & editing Haijun Yan: conceptualization, software. Jianxin Si: methodology, validation, software. Meng Zhang: conceptualization, methodology. Jide Wang: project administration, supervision. Ling Zhao: methodology, supervision. Chao Yang: software, writing – review & editing. Ronglan Wu: conceptualization, supervision.

Conflicts of interest

The authors declare that they have no known competing financial interests or personal relationships that could have appeared to influence the work reported in this paper.

Acknowledgements

The financial support from the National Natural Science Foundation of China (Grant No. 21968033 and U1903130), the Postdoctoral Science Foundation of China (2019M653800), the "Tianshan Youth" Program of Xinjiang Uygur Autonomous Region (2019Q071), the support of 100 Young Doctor Introduction Plan in Xinjiang Uygur Autonomous Region (2016), the Natural Science Foundation of Xinjiang University (BS160222). The authors thank the test platform in the Ministry Key

Laboratory of Oil and Gas Fine Chemicals and State Key Laboratory of Chemistry and Utilization of Carbon Based Energy Resources for assistance with many instruments and testing work. The authors acknowledge facilities and staff at the Physical and Chemical Testing Center of Xinjiang University.

References

1 P. Johnston, N. Carthey and G. J. Hutchings, *J. Am. Chem. Soc.*, 2015, **137**, 14548–14557.
2 G. Malta, S. A. Kondrat, S. J. Freakley, C. J. Davies, S. Dawson, X. Liu, L. Lu, K. Dymkowski, F. Fernandez-Alonso, S. Mukhopadhyay, E. K. Gibson, P. P. Wells, S. F. Parker, C. J. Kiely and G. J. Hutchings, *ACS Catal.*, 2018, **8**, 8493–8505.
3 H. Schobert, *Chem. Rev.*, 2014, **114**, 1743–1760.
4 J. Zhong, Y. Xu and Z. Liu, *Green Chem.*, 2018, **20**, 2412–2427.
5 M. Zhu, Q. Wang, K. Chen, Y. Wang, C. Huang, H. Dai, F. Yu, L. Kang and B. Dai, *ACS Catal.*, 2015, **5**, 5306–5316.
6 J. Oliver-Meseguer, A. Domenech-Carbo, M. Boronat, A. Leyva-Perez and A. Corma, *Angew. Chem., Int. Ed.*, 2017, **56**, 6435–6439.
7 T. K. Mackey, J. T. Contreras and B. A. Liang, *Sci. Total Environ.*, 2014, **472**, 125–129.
8 S. Ali, S. Olanrele, T. Liu, Z. Lian, C. Si, M. Yang and B. Li, *J. Phys. Chem. C*, 2019, **123**, 29203–29208.
9 L. Kang and M. Zhu, *RSC Adv.*, 2019, **9**, 31812–31818.
10 M. Cai, H. Zhang, B. Man, J. Li, L. Li, Y. Li, D. Xie, R. Deng and J. Zhang, *Catal. Sci. Technol.*, 2020, **10**, 3552–3560.
11 Y. Jin, G. Li, J. Zhang, Y. Pu and W. Li, *RSC Adv.*, 2015, **5**, 37774–37779.
12 S. A. Mitchenko, T. V. Krasnyakova, R. S. Mitchenko and A. N. Korduban, *J. Mol. Catal. A: Chem.*, 2007, **275**, 101–108.
13 J. Hu, Q. Yang, L. Yang, Z. Zhang, B. Su, Z. Bao, Q. Ren, H. Xing and S. Dai, *ACS Catal.*, 2015, **5**, 6724–6731.
14 Y. Ren, B. Wu, F. Wang, H. Li, G. Lv, M. Sun and X. Zhang, *Catal. Sci. Technol.*, 2019, **9**, 2868–2878.
15 X. Wang, M. Zhu and B. Dai, *ACS Sustainable Chem. Eng.*, 2019, **7**, 6170–6177.
16 D. Hu, L. Wang, F. Wang and J. Wang, *Chin. Chem. Lett.*, 2018, **29**, 1413–1416.
17 D. Hu, F. Wang and J. Wang, *RSC Adv.*, 2017, **7**, 7567–7575.
18 K. Zhou, J. Jia, X. Li, X. Pang, C. Li, J. Zhou, G. Luo and F. Wei, *Fuel Process. Technol.*, 2013, **108**, 12–18.
19 C. Huang, M. Zhu, L. Kang and B. Dai, *Catal. Commun.*, 2014, **54**, 61–65.
20 G. Li, W. Li and J. Zhang, *Catal. Sci. Technol.*, 2016, **6**, 1821–1828.
21 L. Wang, J. Chen, L. Ge, Z. Zhu and V. Rudolph, *Energy Fuels*, 2011, **25**, 3408–3416.
22 L. Wang, F. Wang and J. Wang, *Catal. Commun.*, 2016, **83**, 9–13.
23 P. Li, M. Ding, L. He, K. Tie, H. Ma, X. Pan and X. Bao, *Sci. China: Chem.*, 2018, **61**, 444–448.
24 S. Wang, B. He, R. Tian, X. Wu, X. An, Y. Liu, J. Su, Z. Yu and X. Xie, *Int. J. Hydrogen Energy*, 2020, **45**, 16409–16420.
25 H. Zhu, J. H. Kwak, C. H. F. Peden and J. Szanyi, *Catal. Today*, 2013, **205**, 16–23.
26 P. Liu, J. Cao, Z. Xu, C. Yang, X. Wang and F. Liu, *Chem. Eng. Sci.*, 2020, **211**, 115273–115282.
27 Z. Song, G. Liu, D. He, X. Pang, Y. Tong, Y. Wu, D. Yuan, Z. Liu and Y. Xu, *Green Chem.*, 2016, **18**, 5994–5998.
28 B. Wang, H. Lai, Y. Yue, G. Sheng, Y. Deng, H. He, L. Guo, J. Zhao and X. Li, *Catalysts*, 2018, **8**, 351–363.
29 L. Wang, F. Wang, J. Wang, X. Tang, Y. Zhao, D. Yang, F. Jia and T. Hao, *React. Kinet., Mech. Catal.*, 2013, **110**, 187–194.
30 L. Wang, F. Wang and J. Wang, *Catal. Commun.*, 2015, **65**, 41–45.
31 L. Wang, F. Wang and J. Wang, *New J. Chem.*, 2016, **40**, 3019–3023.
32 L. Wang, L. Lian, H. Yan, F. Wang, J. Wang, C. Yang and L. Ma, *RSC Adv.*, 2019, **9**, 30335–30339.
33 X. Li, Y. Nian, S. Shang, H. Zhang, J. Zhang, Y. Han and W. Li, *Catal. Sci. Technol.*, 2019, **9**, 188–198.
34 J. Zhao, B. Wang, Y. Yue, G. Sheng, H. Lai, S. Wang, L. Yu, Q. Zhang, F. Feng, Z.-T. Hu and X. Li, *J. Catal.*, 2019, **373**, 240–249.
35 Y. Yu, Y. Yue, B. Wang, H. He, Z.-T. Hu, J. Zhao and X. Li, *Catalysts*, 2019, **9**, 1–22.
36 X. Qiao, C. Zhao, Z. Zhou, Q. Guan and W. Li, *ACS Sustainable Chem. Eng.*, 2019, **7**, 17979–17989.
37 J. Zhao, T. Zhang, X. Di, J. Xu, J. Xu, F. Feng, J. Ni and X. Li, *RSC Adv.*, 2015, **5**, 6925–6931.
38 H. Li, B. Wu, F. Wang and X. Zhang, *ChemCatChem*, 2018, **10**, 4090–4099.
39 Y. Han, H. Zhang, Y. Li, Y. Nian, W. Li and J. Zhang, *Catal. Today*, 2020, **355**, 205–213.
40 A. Romero, A. Santos, J. Tojo and A. Rodriguez, *J. Hazard. Mater.*, 2008, **151**, 268–273.
41 A. P. Abbott, G. Capper, D. L. Davies, R. K. Rasheed and V. Tambyrajah, *Green Chem.*, 2002, **4**, 24–26.
42 R. Calderon Morales, V. Tambyrajah, P. R. Jenkins, D. L. Davies and A. P. Abbott, *Chem. Commun.*, 2004, **2**, 158–159.
43 K. Haerens, E. Matthijs, K. Binnemans and B. Van der Bruggen, *Green Chem.*, 2009, **11**, 1357–1365.
44 C.-M. Lin, R. B. Leron, A. R. Caparanga and M.-H. Li, *J. Chem. Thermodyn.*, 2014, **68**, 216–220.
45 G. Kresse and J. Furthmüller, *Comput. Mater. Sci.*, 1996, **6**, 15–50.
46 G. Kresse and J. Furthmüller, *Phys. Rev. B: Condens. Matter Mater. Phys.*, 1996, **54**, 11169–11186.
47 J. P. Perdew, K. Burke and M. Ernzerhof, *Phys. Rev. Lett.*, 1996, **77**, 3865–3868.
48 P. E. Blöchl, *Phys. Rev. B: Condens. Matter Mater. Phys.*, 1994, **50**, 17953–17979.
49 G. Kresse and D. Joubert, *Phys. Rev. B: Condens. Matter Mater. Phys.*, 1999, **59**, 1758–1775.
50 X. Chen, Q. Xu, B. Zhao, S. Ren, Z. Wu, J. Wu, Y. Yue, D. Han and R. Li, *Catal. Lett.*, 2021, **151**, 3372–3380.
51 G. Lan, Y. Yang, X. Wang, W. Han, H. Tang, H. Liu and Y. Li, *Microporous Mesoporous Mater.*, 2018, **264**, 248–253.

52 B. Wang, Y. Yue, C. Jin, J. Lu, S. Wang, L. Yu, L. Guo, R. Li, Z.-T. Hu, Z. Pan, J. Zhao and X. Li, *Appl. Catal., B*, 2020, **272**, 118944–118954.
53 Q. L. Song, S. J. Wang, B. X. Shen and J. G. Zhao, *Pet. Sci. Technol.*, 2010, **28**, 1825–1833.
54 X. Qi, W. Chen and J. Zhang, *RSC Adv.*, 2019, **9**, 21931–21938.
55 L. Yang, Q. Yang, J. Hu, Z. Bao, B. Su, Z. Zhang, Q. Ren and H. Xing, *AIChE J.*, 2018, **64**, 2536–2544.
56 H. He, J. Zhao, B. Wang, Y. Yue, G. Sheng, Q. Wang, L. Yu, Z.-T. Hu and X. Li, *RSC Adv.*, 2019, **9**, 21557–21563.
57 M. Zhang, L. Wang, H. J. Yan, L. Z. Lian, J. X. Si, Z. Q. Long, X. X. Cui, J. D. Wang, L. Zhao, C. Yang, R. L. Wu and L. D. Ma, *J. Mater. Res. Technol.*, 2021, **13**, 2055–2065.
58 Z. Shen, Y. Liu, Y. Han, Y. Qin, J. Li, P. Xing and B. Jiang, *RSC Adv.*, 2020, **10**, 14556–14569.
59 Y. Lu, F. Lu and M. Zhu, *J. Taiwan Inst. Chem. Eng.*, 2020, **113**, 198–203.
60 F. Lu, Y. Lu, M. Zhu and B. Dai, *ChemistrySelect*, 2020, **5**, 878–885.
61 Y. Wang, Y. Nian, J. Zhang, W. Li and Y. Han, *Mol. Catal.*, 2019, **479**, 110612–110622.
62 C. Zhang, H. Zhang, Y. Li, L. Xu, J. Li, L. Li, M. Cai and J. Zhang, *ChemCatChem*, 2019, **11**, 3441–3450.
63 Y. Shi, Z. Li, J. Wang and R. Zhou, *Appl. Catal., B*, 2021, **286**, 119936–119945.
64 Y. Liu, H. Zhang, X. Li, L. Wang, Y. Dong, W. Li and J. Zhang, *Appl. Catal., A*, 2021, **611**, 117902–117913.
65 W. Kiatkittipong, S. Wongsakulphasatch, N. Tintan, N. Laosiripojana, P. Praserthdam and S. Assabumrungrat, *Fuel Process. Technol.*, 2011, **92**, 1999–2004.
66 H. Naseri, G. Mazloom, A. Akbari and F. Banisharif, *Microporous Mesoporous Mater.*, 2021, **325**, 11341–11352.
67 Y. Aponte and H. de Lasa, *Ind. Eng. Chem. Res.*, 2017, **56**, 1948–1960.
68 X. L. Qiao, X. Y. Liu, Z. Q. Zhou, Q. X. Guan and W. Li, *Catal. Sci. Technol.*, 2021, **11**, 2327–2339.
69 Z. Chen, P. Zou, R. Zhang, L. Dai and Y. Wang, *Catal. Lett.*, 2015, **145**, 2029–2036.
70 S. Hu, D. Liu, L. Li, Z. Guo, Y. Chen, A. Borgna and Y. Yang, *Chem. Eng. J.*, 2010, **165**, 916–923.
71 J. Pedada, H. B. Friedrich and S. Singh, *J. Iran. Chem. Soc.*, 2018, **15**, 1411–1418.
72 J. Zhao, S. Wang, B. Wang, Y. Yue, C. Jin, J. Lu, Z. Fang, X. Pang, F. Feng, L. Guo, Z. Pan and X. Li, *Chin. J. Catal.*, 2021, **42**, 334–346.
73 X. Wang, G. Lan, Z. Cheng, W. Han, H. Tang, H. Liu and Y. Li, *Chin. J. Catal.*, 2020, **41**, 1683–1691.
74 H. He, J. Zhao, B. Wang, Y. Yue, G. Sheng, Q. Wang, L. Yu, Z. T. Hu and X. Li, *Materials*, 2019, **12**, 1310–1322.
75 J. Gu, Y. Gao, J. Zhang, W. Li, Y. Dong and Y. Han, *Catalysts*, 2017, **7**, 17–29.
76 L. Hou, J. Zhang, Y. Pu and W. Li, *RSC Adv.*, 2016, **6**, 18026–18032.
77 X. Li, J. Zhang and W. Li, *J. Ind. Eng. Chem.*, 2016, **44**, 146–154.